Asian Journal of Chemistry; Vol. 33, No. 4 (2021), 807-813

ASIAN JOURNAL OF CHEMISTRY

https://doi.org/10.14233/ajchem.2021.23083

Crystal Structure and Infrared Spectroscopy of *trans*-$[Cr(NCS)_2(Me_2tn)_2][Cr(NCS)_4(Me_2tn)]$ Moiety

DOHYUN MOON[1] and JONG-HA CHOI[2,*]

[1]Pohang Accelerator Laboratory, POSTECH, Pohang 37673, Republic of Korea
[2]Department of Chemistry andong National University, Andong 36729, Republic of Korea

*Corresponding author: E-mail: jhchoi@anu.ac.kr

Received: 30 November 2020; *Accepted*: 3 February 2021; *Published online*: 20 March 2021; AJC-20287

A novel double complex, *trans*-$[Cr(NCS)_2(Me_2tn)_2][Cr(NCS)_4(Me_2tn)]\cdot NaSCN\cdot$*i*-PrOH, (**1**) ($Me_2tn$ = 2,2-dimethyl-1,3-propanediamine, $C_5H_{14}N_2$; *i*-PrOH = isopropyl alcohol), was prepared and its structure was determined by single-crystal X-ray diffraction at 95 K. The complex **1** crystallized in the space group $P\bar{1}$ of the triclinic system with two nuclear formula units in a cell of dimensions a = 13.220(3), b = 13.699(3), c = 15.087(3) Å and α = 116.193(3), β = 102.73(3) and γ = 104.48(3)°. X-ray structural analysis revealed two crystallographically independent Cr(III) complex cations in the complex **1**. The asymmetric unit contains two halves of *trans*-$[Cr(NCS)_2(Me_2tn)_2]^+$ cations (**2** and **3**), one *cis*-$[Cr(NCS)_4(Me_2tn)]^-$ anion (**4**), one NaSCN salt and one isopropyl alcohol molecule. In two independent complex cations, the chromium(III) ions are coordinated by four N atoms of two chelating Me_2tn and two NCS groups in a distorted octahedral geometry while the chromium(III) ion in *cis*-$[Cr(NCS)_4(Me_2tn)]^-$ has a distorted octahedral coordination with two N atoms of one Me_2tn and four NCS groups. The two six-membered rings in *trans*-$[Cr(NCS)_2(Me_2tn)_2]^+$ cations adopt both *anti* chair-chair conformations. The Cr–N(Me_2tn) bond lengths range from 2.0624(18) to 2.0877(16) Å, while the Cr–N(NCS) bond lengths range from 2.0718(16) to 2.0428 (16) Å. The crystal lattice is stabilized by hydrogen bonding interactions among the NH groups of the Me_2tn ligand, OH group of *i*-PrOH and the S atoms of the NCS groups. The infrared spectral properties are also described.

Keywords: Double chromium(III) complex, Crystal structure, 2,2-Dimethyl-1,3-propanediamine, Thioncyanato group.

INTRODUCTION

2,2-Dimethyl-1,3-propanediamine (Me_2tn) can coordinate with a central cobalt(III) or chromium(III) ion through its two nitrogen atoms as a bidentate ligand, thereby forming a six-membered chelate ring [1]. Geometric and conformational isomerism of coordination compounds formed by two N donor Me_2tn ligands is an interesting field. The six-membered chelate ring can adopt a chair, skewed boat (twist) or boat conformation [2]. The $[CrL_2(Me_2tn)_2]^+$ (L = monodentate ligand) cation can exist either as the *trans* or *cis* isomer. The *trans*-isomer can also adopt two different types of conformations with respect to the chelate rings of the Me_2tn ligand (Fig. 1). The carbon atoms of the two six-membered chelate rings of each conformer can be present on the same side (*syn* conformer) or on the opposite side (*anti* conformer) of the equatorial Me_2tn coordination plane. In addition to these stable species, there are more strained conformers with chelate rings in boat or twist-boat conformations. Furthermore, the NCS group may coordinate to a transition metal through the nitrogen or the sulfur or both. The oxidation state of the metal, the nature of other ligands in a complex and steric factor also influence the mode of coordination. The infrared, electronic absorption and emission spectral properties are valuable tools in distinguishing between isothioncyanato (M-NCS), thioncyanato (M-SCN) and bridging thioncyanato (M-NCS-M) complexes [3]. However, the infrared and visible absorption data do not give definite evidence whether *trans*-$[Cr(NCS)_2(Me_2tn)_2]^+$ is *syn* or *anti* conformer of the six-membered chelate rings. It also should be noted that the geometric and conformational assignments based on spectral data are not always conclusive [4].

The X-ray structural analyses of *trans-anti*-$[CrCl_2(Me_2tn)_2]ClO_4$ [5], *trans-anti*-$[CrBr_2(Me_2tn)_2]ClO_4$ [6], *trans-anti*-$[CrCl_2(Me_2tn)_2]_2ZnCl_4$ [7], *trans-anti*-$[Cr(NCS)_2(Me_2tn)_2]SCN\cdot 0.5H_2O$ [4], *trans-anti*-$[Cr(N_3)_2(Me_2tn)_2]ClO_4\cdot 2H_2O$ [8] and *trans-anti*-$[Cr(OH)(H_2O)(Me_2tn)_2](ClO_4)_2$ [9] revealed that the

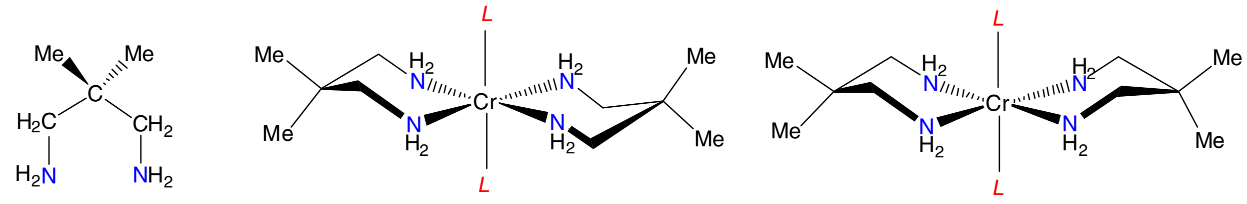

Me_2tn = 2,2-dimethyl-1,3-propanediamine *anti* conformer *syn* conformer

Fig. 1. Chemical structure of Me_2tn and two possible conformers of *trans*-$[CrL_2(Me_2tn)_2]^+$

two chelate rings of Me_2tn ligands adopt only the *anti* chair-chair conformation. However, in case of *trans-anti*-$[CrCl_2(Me_2tn)_2]_{1.5}$-[*syn*-$CrBr_2(Me_2tn)_2]_{0.5}Br_2$, *trans-anti/syn*-$[CrBr_2(Me_2tn)_2]_2ZnBr_4$ [10], *trans-anti/syn*-$[CrCl_2(Me_2tn)_2]Cl$ [11], *trans-anti/syn*-$[CrBr_2(Me_2tn)_2]Br$ [12], *trans-anti/syn*-$[CrBr_2(Me_2tn)_2]_2Br_2{\cdot}HClO_4{\cdot}H_2O$ [13] and *trans-anti/syn*-$[Cr(N_3)_2(Me_2tn)_2]_3[Cr(N_3)_4(Me_2tn)]_2ClO_4$ [14], both *syn* and *anti* conformers were observed within the same single crystal. Two chelate rings of Me_2tn ligands in *trans-syn*-$[Cr(N_3)_{0.8}Cl_{1.2}(Me_2tn)_2]ClO_4$ adopted the *syn* chair-chair conformation [15]. In addition, *cis*-$[Cr(NCS)_2(Me_2tn)_2]Br$ and *cis*-$[CrBr(NCS)(Me_2tn)_2]$[*trans-anti*-$CrBr_2(Me_2tn)_2]Br_2$ were synthesized and characterized by IR spectroscopy and *X*-ray crystallography [10]. The different arrangements of the two six-membered chelate rings of Me_2tn ligands may be dependent on the crystal packing force and the presence of hydrate molecules, co-crystallizing salt and counter anions. It is observed that the factors determining the stability of two conformers are indistinct and more complicated. Thus, the elucidation of the factors stabilizing either the *syn* or *anti* conformation has gained research attention.

In present work, the synthesis of a new complex, *trans*-$[Cr(NCS)_2(Me_2tn)_2][Cr(NCS)_4(Me_2tn)]{\cdot}NaSCN{\cdot}$*i*-PrOH (**1**), vibrational spectral properties and structural characterization by synchrotron single-crystal X-ray diffraction are reported.

EXPERIMENTAL

All the chemicals were of reagent grade materials and used without further purification. The mid-infrared spectrum was obtained from KBr pellets with a JASCO 460 plus series FT-IR spectrometer. Analyses for C, H and N were conducted on a Carlo-Erba 1108 Elemental Vario EL analyzer.

As starting material, *trans*-$[CrCl_2(Me_2tn)_2]Cl$ was synthesized as described in literature [1]. Elemental analysis of calcd. (found) % of $C_{10}H_{28}N_4Cl_3Cr$: C, 33.11 (33.42); H, 7.78 (8.90); N, 15.45 (15.64). A solution of potassium thiocyante (1.0 g, 0.01 mol) in water (20 mL) was added to a solution of *trans*-$[CrCl_2(Me_2tn)_2]Cl$ (0.36 g, 1.0 mmol) in hot acetic acid (40 mL, 0.1 M). The solution was heated at 80 °C for 20 min during which time the colour of the solution changed from green to red. The *trans*-$[Cr(NCS)_2(Me_2tn)_2]SCN{\cdot}0.5H_2O$ which formed was dissolved in mixed solvent 20 mL with water and isopropyl alcohol and followed by precipitation with a saturated solution of sodium perchlorate. The resulting solution was allowed to stand at room temperature for a few days to give red crystals of complex **1** suitable for synchrotron X-ray structural analysis. Elemental analysis of calcd. (found) % of $C_{26}H_{52}Cr_2N_{13}NaOS_7$: C, 34.16 (32.45); H, 5.73 (6.10); N, 19.92 (15.56). IR (KBr, cm^{-1}): 3466 br (ν OH), 3244 sh, 3200 vs and 3116 vs (ν NH), 2961 vs, 2933 m, 2914 sh and 2875 vs (ν CH), 2126 vs (ν CN), 2093 vs, 2072 vs and 2040 vs (ν CN), 1617 m, 1579 vs (δ NH_2), 1475 vs and 1467 sh (δ_{as} CH_2), 1416 vs, 1383 m and 1373 sh (δ_s CH_2), 1342 m and 1326 s (ω NH_2), 1279 s (ω CH_2), 1213 vs, 1153 vs (γ NH_2), 1137 s (ν CN), 1041 vs (ν CN), 989 vs (ν CC), 950 m, 895 s (ρ NH_2), 774 vs (ρ CH_2), 670 s and 658 vs, 553 vs (ν CrN + ring def.), 501 m, 482 m (δ NCS), 452 m and 420 vs (ν CrN).

X-ray structural determination: A crystal of complex **1** was coated with Parabar 10312 (Hampton Research Inc.) and the diffraction data measured at 95(2) K with synchrotron radiation ($\lambda = 0.66999$ Å) on an ADSC Quantum-210 detector at 2D SMC with a silicon (111) double crystal monochromator (DCM) at the Pohang Accelerator Laboratory, Korea. The PAL BL2D-SMDC program [16] was used for data collection and HKL3000sm (Ver. 720) [17] was used for cell refinement, reduction and absorption correction. The crystal structure of complex **1** was solved by the intrinsic phasing method with SHELXT [18] and refined by full-matrix least-squares calculations with the SHELXL program [19]. All non-hydrogen atoms and all the solvent atoms were refined anisotropically. Molecular graphics were produced using DIAMOND-3 [20]. The hydrogen atoms were assigned isotropic displacement coefficients $U(H) = 1.2U(C, N)$ or $1.5U(C_{methyl})$ and their coordinates were allowed to ride on their respective atoms. Refinement of the structure converged at a final $R_1 = 0.0500$, $wR_2 = 0.1435$ for 14564 reflections with $I > 2\sigma(I)$; $R_1 = 0.0534$, $wR_2 = 0.1462$ for all reflections. The largest difference peak and hole were 1.952 and -1.100 e $Å^{-3}$, respectively. Crystal data, data collection and structure refinement details are summarized in Table-1. CCDC-2046923 contains the supplementary crystallographic data for this paper. The data can be obtained free of charge at www.ccdc.cam.ac.uk/conts/retrieving.htmL or from the Cambridge Crystallographic Data Centre, 12, Union Road, Cambridge CB2 1EX, UK.

RESULTS AND DISCUSSION

Infrared spectroscopy: The IR spectrum of *trans*-isomer reveal a simpler pattern than that of *cis*-isomer and this pattern may be rationalized on the basis of the higher symmetry of the *trans*-isomer [3,7-15]. The FT-IR spectrum of complex **1** is depicted in Fig. 2.

The resulting wavenumbers, intensities and assignments of the principal IR bands are also summarized in Table-2. The tentative assignments were made according to the literature

TABLE-1
CRYSTALLOGRAPHIC DATA FOR COMPLEX **1**

Crystal data	
Chemical formula	$[Cr(NCS)_2(C_5H_{14}N_2)_2][Cr(NCS)_4(C_5H_{14}N_2)]\cdot NaSCN\cdot$*i*-PrOH
M_r	914.22
Crystal system, space group	Triclinic, $P\bar{1}$
Temperature (K)	95
a, b, c (Å)	13.220(3), 13.699(3), 15.087(3)
α, β, γ (°)	116.193(3), 102.73(3), 104.48(3)
V (Å^3)	2195.3(8)
Z	2
Radiation type	Synchrotron, λ = 0.66999 Å
μ (mm^{-1})	0.69
Crystal size (mm)	0.21 × 0.20 × 0.18
Data collection	
Diffractometer	ADSC Q210 CCD area detector diffractometer
Absorption correction	Empirical (using intensity measurements) (HKL3000 SCALEPACK)
T_{min}, T_{max}	0.869, 0.887
No. of measured, independent and observed [I > 2σ(I)] reflections	28658, 14564, 13318
R_{int}	0.018
$(\sin \theta/\lambda)_{max}$ (Å^{-1})	0.746
Refinement	
$R[F^2 > 2\sigma(F^2)]$, $wR(F^2)$, S	0.050, 0.146, 1.05
Number of reflections	14654
Number of parameters	540
Number of restraints	56
H-atom treatment	H atoms parameters constrained
$\Delta\rho_{max}$, $\Delta\rho_{min}$ (e Å^{-3})	1.95, –1.10

TABLE-2
ASSIGNMENTS OF THE SELECTED BANDS OCCURRING IN THE IR SPECTRUM OF COMPLEX **1**

Frequency (cm^{-1})	Assignment	Frequency (cm^{-1})	Assignment
3466 br	ν(OH)	1137 s	γ(CH_2)
3244 sh, 3200 vs, 3116 vs	ν(NH)	1041 vs	ν(CO) + ν(CN)
2961 vs, 2933 m, 2914 m, 2875 s	ν(CH)	989 vs	ν(CC)
2126 vs, 2093 vs, 2072 vs, 2040 vs	ν(CN)	950 m	
1617 m		895 s	ρ(CH_2)
1579 vs	δ(NH_2)	774 vs	ρ(NH_2)
1475 vs, 1467 sh	δ_{as}(CH_2)	670 s, 658 vs	
1416 vs		636 vs	
1383 m, 1373 sh	δ_s(CH_2)	553 vs	ν(CrN) + ring def.
1342 m, 1326 s	ω(NH_2)	501 m	
1279 s	ω(CH_2)	482 m	δ(NCS)
1213 vs		452 m	ν(CrN)
1153 vs	γ(NH_2)	420 vs	ν(CrN)

data [7-15]. The broad band at 3466 cm^{-1} can be attributed to the ν(OH) of the surface moisture on the KBr disc or isopropyl alcohol. The strong absorptions at 3250-3100 cm^{-1} and 2970-2850 cm^{-1} are assigned to N–H and C–H stretching modes, respectively. The *N*-bonded thiocyanato ligand displays a ν(CN) near 2050 cm^{-1} [3]. The strong bands observed in the 2150–2040 cm^{-1} region correspond to the ν(CN) vibration of thiocyanate anion and *N*-bonded thiocyanato group. The δ(NCS) bending mode appears as a medium band at 482 cm^{-1} [3]. The positions of the ν(CN), ν(CS) and δ(NCS) modes could be also determined by comparing the IR spectra of the corresponding chloro and bromo complexes which the bands are absent. The $(CH_2)_n$ groups in the compound are reported to display broad absorption bands for scissoring (δ) (1500-1400 cm^{-1}), wagging (ω) (1382-1170 cm^{-1}), twisting (γ) (1295-1063 cm^{-1}) and rocking

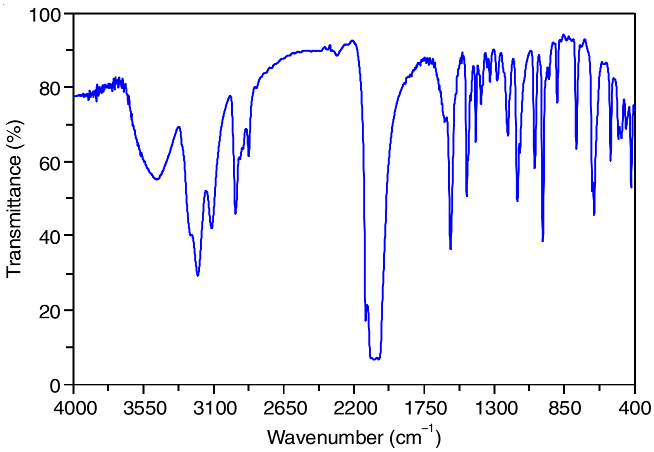

Fig. 2. FT-IR spectrum of complex **1**

(ρ) (1174-724 cm^{-1}) motions [3]. In complex **1**, the strong absorption band at 1480-1420 cm^{-1} can be assigned to CH_2 scissoring. The CH_2 wagging and twisting vibrations, as well as the ν(CC) and ν(CN) modes, were found to occur at 1400–1000 cm^{-1}. The strong absorption band at 1570 cm^{-1} can be attributed to the NH_2 scissoring mode, while the bands at 1475 and 1467 cm^{-1} are ascribed to the CH_2 bending modes. The peak corresponding to CH_2 deformation was observed at 1416 cm^{-1}. The presence of methyl and methylene groups in Me_2tn ligand can be verified by analyzing the region from 1485 to 1360 cm^{-1}. The absorption bands at 1383 and 1373 cm^{-1} are due to the bending modes of CH_3. The strong absorption band at 1279 cm^{-1} is assigned to the CH_2 wagging mode, while the medium to weak absorption bands at 1342 and 1326 cm^{-1} can be assigned to the NH_2 wagging modes. The two strong absorption bands at 1153 and 1137 cm^{-1} are due to the NH_2 and CH_2 twisting modes, respectively. The strong absorption band at 1041 cm^{-1} can be assigned to the skeletal modes involving C–O and C–N stretching. The positions of absorption bands corresponding to the scissoring (δ), wagging (ω), twisting (γ) and rocking (ρ) modes of the NH_2 and CH_2 deformations are not significantly affected by the differing counter anions [7-15]. The strong absorption band at 989 cm^{-1} corresponds to the C–C stretching mode. It has been suggested that the *cis* isomer exhibits at least three bands in the 900-870 cm^{-1} region that can be attributed to the CH_2 rocking mode, while the NH_2 rocking vibration results in the splitting of the peak into two in the 830-760 cm^{-1} region. However, the *trans* isomer shows two groups of bands: one group near 890 cm^{-1}, ascribed to the methylene vibration and a doublet near 800 cm^{-1}, which is mainly due to the amine vibration [7-15]. Complex **1** exhibits one band at 895 cm^{-1} in the NH_2 rocking frequency region, while the band ascribed to CH_2 rocking are observed at 774 cm^{-1}. Metal-ligand stretching bands occur in the far-IR range. Bands in the 560-400 cm^{-1} region are of interest because they can be used to distinguish the *cis* and *trans*-isomers of diacidobis(diamine)chromium(III) complexes. All *trans* complexes show three bands in this region, whereas all *cis* complexes show four strong bands [7-15]. In the far-IR spectral range of the *trans*-$[Cr(NCS)_2N_4]^+$ complex with the D_{4h} symmetry, the group theory analysis predicts two Cr–N and one Cr–NCS stretching vibrations. Complex **1** shows a pattern of three bands: one strong band at 530 cm^{-1} and two other medium bands at 452 and 420 cm^{-1}, wherein the latter can be assigned to the Cr–N stretching modes. Therefore, the IR spectral properties of complex **1** confirm the existence of the *trans* configurational geometry. However, the IR spectral data do not provide any evidence on whether the two six-membered chelate rings of *trans*-$[Cr(NCS)_2(Me_2tn)_2]^+$ adopt the *syn* or *anti* conformation.

Crystal structure: To unambiguously determine the conformations of the six-membered chelate rings, the single-crystal structure analysis was performed using a synchrotron X-ray system. Complex **1** crystallizes in the triclinic space group of $P\bar{1}$, with two formula units in a cell having the dimensions of $a = 13.220(3)$, $b = 13.699(3)$, $c = 15.087(3)$ Å and $\alpha = 116.193(3)$, $\beta = 102.73(3)$ and $\gamma = 104.48(3)°$. The complex is another example of *trans*-$[Cr(NCS)_2(Me_2tn)_2]^+$; however, Cr(III) complex counter anion used here including NaSCN and *i*-PrOH exhibits some interesting structural features. X-ray structural analysis revealed that there are two crystallographically independent Cr(III) complex cations in complex **1**. In two complex cations, Cr(III) ions are coordinated by four N atoms of two chelating Me_2tn ligands and two NCS groups in a *trans* arrangement, displaying a distorted octahedral geometry. The asymmetric unit contains two halves of centrosymmetric $[Cr1(NCS)_2(Me_2tn)_2]^+$ (**2**) and $[Cr2(NCS)_2(Me_2tn)_2]^+$ (**3**) cations, one $[Cr3(NCS)(Me_2tn)_4]^-$ (**4**) anion, one NaSCN salt and one *i*-PrOH molecule. The Cr1 and Cr2 complex cations are in half occupancy in the asymmetric unit: each molecule contributes a charge of +0.5. The ellipsoid plots of two complex cations **2** and **3** and complex anion **4**, along with atomic labeling, are illustrated in Figs. 3-5. Selected bond lengths and angles are listed in Tables 3 and 4, respectively. In Figs. 3-5, the hydrogen atoms are shown as circles with arbitrary radii and the disordered NCS groups are omitted for clarity. The Cr1 and Cr2 atoms are located at crystallographic center of symmetry; thus, two Cr complex cations have the molecular C_i symmetry. All six-membered rings formed by the Me_2tn ligand adopt the most stable chair conformations.

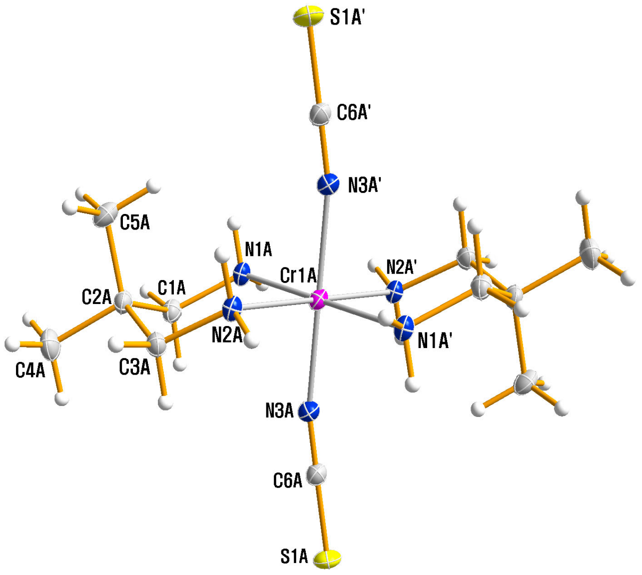

Fig. 3. Molecular structure of **2** in complex **1**. The displacement ellipsoids are shown at the 50% probability level and the disordered NCS groups are omitted for clarity. The atoms labeled with prime symbols are related by symmetry code (–*x*, –*y*+2, *z*+1)

In the $[Cr1(NCS)_2(Me_2tn)_2]^+$ (**2**) and $[Cr2(NCS)_2(Me_2tn)_2]^+$ (**3**) cations, the Cr(III) centers are coplanar with the four N atoms and they adopt a distorted octahedral geometry. The four nitrogen atoms of the two bidentate Me_2tn ligands occupy the equatorial sites and the two NCS ligands coordinate with the Cr(III) metal center in the *trans*-arrangement. The two chelate rings of the Me_2tn ligands in complexes **2** and **3** adopt the *anti* chair-chair conformation. The conformational arrangements of complexes **2** and **3** are consistent with the *anti* conformation arrangement observed for *trans*-*anti*-$[CrCl_2(Me_2tn)_2]ClO_4$ [5], *trans*-*anti*-$[CrCl_2(Me_2tn)_2]_2ZnCl_4$ [7], *trans*-*anti*-$[Cr(NCS)_2$-

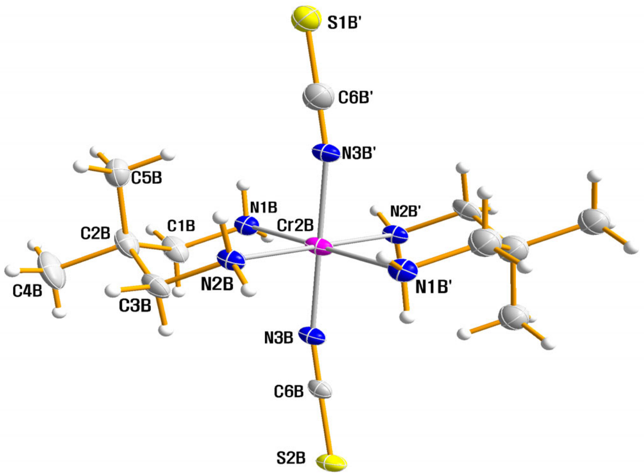

Fig. 4. Molecular structure of **3** in complex **1**. The displacement ellipsoids are shown at the 50% probability level. The atoms labeled with prime symbols are related by symmetry code ($-x+1$, $-y+1$, $-z+2$)

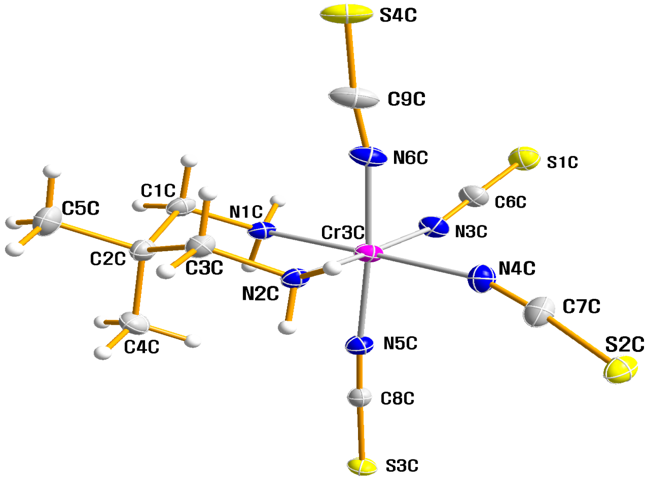

Fig. 5. Molecular structure of **4** in complex **1**. The displacement ellipsoids are shown at the 50% probability level and the disordered NCS groups are omitted for clarity

TABLE-3
SELECTED BOND DISTANCES (Å) FOR COMPLEX **1**

Cr1A—N3A	1.9895 (17)	N3B—C6B	1.168 (2)	N1C—C1C	1.492 (3)
Cr1A—N1A	2.0718 (16)	Cr3C—N6C	1.9869 (18)	N2C—C3C	1.488 (2)
Cr1A—N2A	2.0877 (16)	Cr3C—N3C	2.003 (2)	N3C—C6C	1.167 (3)
S1A—C6A	1.618 (2)	Cr3C—N5C	2.0095 (18)	N4C—C7C	1.169 (3)
S1D—C6A	1.661 (19)	Cr3C—N4C	2.0112 (19)	N5C—C8C	1.168 (3)
N1A—C1A	1.484 (2)	Cr3C—N2C	2.0624 (18)	N6C—C9C	1.164 (3)
N2A—C3A	1.491 (2)	Cr3C—N1C	2.0634 (17)	S1S—C1S	1.653 (3)
N3A—C6A	1.173 (2)	S1C—C6C	1.615 (5)	N1S—C1S	1.167 (4)
Cr2B—N3B	1.9857 (17)	S2C—C7C	1.679 (7)	S2S—C2S	1.49 (4)
Cr2B—N2B	2.0719 (17)	S3C—C8C	1.630 (2)	N2S—C2S	1.24 (5)
Cr2B—N1B	2.084 (2)	S4C—C9C	1.589 (4)	O1I—C1I	1.401 (6)
S2B—C6B	1.619 (2)	S1F—C6C	1.642 (13)	C1I—C2I	1.401 (8)
N1B—C1B	1.484 (3)	S2F—C7C	1.584 (5)	C2I—C3I	1.486 (9)
N2B—C3B	1.492 (3)	S4F—C9C	1.694 (5)	C2I—C4I	1.497 (10)

TABLE-4
SELECTED BOND ANGLES (°) FOR COMPLEX **1**

N3A^{i}—Cr1A—N3A	180.00 (10)	N3B^{ii}—Cr2B—N1B	88.58 (8)	C3C—N2C—Cr3C	121.65 (12)
N3A^{i}—Cr1A—N1A	89.18 (7)	N2B—Cr2B—N1B	92.31 (8)	C6C—N3C—Cr3C	157.31 (18)
N3A—Cr1A—N1A	90.82 (7)	N1B^{ii}—Cr2B—N1B	180.0	C7C—N4C—Cr3C	161.64 (18)
N1A—Cr1A—N1A^{i}	180.0	C1B—N1B—Cr2B	120.93 (14)	C8C—N5C—Cr3C	175.83 (15)
N3A^{i}—Cr1A—N2A	88.67 (7)	C3B—N2B—Cr2B	118.56 (13)	C9C—N6C—Cr3C	169.5 (2)
N3A—Cr1A—N2A	91.33 (7)	C6B—N3B—Cr2B	164.75 (17)	N1C—C1C—C2C	114.25 (15)
N1A—Cr1A—N2A	90.66 (7)	N1B—C1B—C2B	115.23 (17)	N3C—C6C—S1C	177.0 (3)
N1A^{i}—Cr1A—N2A	89.34 (7)	N6C—Cr3C—N3C	89.95 (8)	N3C—C6C—S1F	174.3 (15)
N2A—Cr1A—N2A^{i}	179.999 (1)	N6C—Cr3C—N5C	175.78 (8)	S1C—C6C—S1F	8.5 (14)
C1A—N1A—Cr1A	119.10 (11)	N3C—Cr3C—N5C	92.30 (8)	N4C—C7C—S2F	173.0 (11)
C3A—N2A—Cr1A	119.07 (12)	N6C—Cr3C—N4C	93.57 (8)	N4C—C7C—S2C	174.7 (3)
C6A—N3A—Cr1A	168.08 (15)	N3C—Cr3C—N4C	92.31 (9)	S2F—C7C—S2C	12.1 (9)
N1A—C1A—C2A	115.28 (15)	N5C—Cr3C—N4C	89.91 (8)	N5C—C8C—S3C	178.56 (18)
N3A—C6A—S1A	179.2 (2)	N6C—Cr3C—N2C	86.75 (7)	N6C—C9C—S4C	173.2 (5)
N3A—C6A—S1D	166 (3)	N3C—Cr3C—N2C	176.27 (7)	N6C—C9C—S4F	170.4 (6)
S1A—C6A—S1D	15 (2)	N5C—Cr3C—N2C	91.10 (7)	S4C—C9C—S4F	16.40 (17)
N3B—Cr2B—N3B^{ii}	180.00 (11)	N4C—Cr3C—N2C	86.16 (8)	N1S—C1S—S1S	177.7 (2)
N3B—Cr2B—N2B	88.81 (7)	N6C—Cr3C—N1C	87.08 (7)	N2S—C2S—S2S	174 (3)
N3B^{ii}—Cr2B—N2B	91.19 (7)	N3C—Cr3C—N1C	88.86 (8)	O1I—C1I—C2I	162.4 (5)
N2B—Cr2B—N2B^{ii}	179.999 (1)	N5C—Cr3C—N1C	89.40 (7)	C1I—C2I—C3I	110.7 (5)
N3B—Cr2B—N1B^{ii}	88.58 (8)	N4C—Cr3C—N1C	178.66 (7)	C1I—C2I—C4I	117.0 (7)
N2B—Cr2B—N1B^{ii}	87.69 (8)	N2C—Cr3C—N1C	92.70 (8)	C3I—C2I—C4I	100.1 (6)
N3B—Cr2B—N1B	91.42 (8)	C1C—N1C—Cr3C	120.89 (12)		

Symmetry codes: (i) $-x$, $-y+2$, $-z+1$; (ii) $-x+1$, $-y+1$, $-z+2$.

$(Me_2tn)_2]SCN{\cdot}0.5H_2O$ [4] and *trans-anti*-$[Cr(N_3)_2(Me_2tn)_2]ClO_4{\cdot}2H_2O$ [8]. The same *anti* conformational arrangements are comparable to the *syn* conformation observed for *trans-anti/syn*-$[CrCl_2(Me_2tn)_2]Cl$ [11], *trans-anti/syn*-$[CrBr_2(Me_2tn)_2]Br$ [12], *trans-anti/syn*-$[CrBr_2(Me_2tn)_2]_2Br_2{\cdot}HClO_4{\cdot}H_2O$ [13], *trans-anti/syn*-$[Cr(N_3)_2(Me_2tn)_2]_3[Cr(N_3)_4(Me_2tn)]_2ClO_4$ [14] and *trans-syn*-$[CrCl_{1.2}(N_3)_{0.8}(Me_2tn)_2]ClO_4$ [15]. The observed differences in the conformations of the two chelate rings arise from the differences in the crystal packing and hydrogen-bonding forces among the solvent molecules, complex cations, co-crystal salt and anions in the complexes. The Cr–N bond distances for the nitrogen atoms of Me_2tn vary from 2.0624(18) to 2.0877(16) Å, are very close to the corresponding bond distances reported for *trans-anti*-$[CrCl_2(Me_2tn)_2]ClO_4$ [5], *trans-anti*-$[CrCl_2(Me_2tn)_2]_2ZnCl_4$ [7], *trans-anti*-$[Cr(N_3)_2(Me_2tn)_2]ClO_4{\cdot}2H_2O$ [8], *trans*-[Cr(nic-*O*)$_2$(cyclam)]ClO_4 [21] and [Cr(ox)(cyclam)]ClO_4 [22]. The Cr–NCS bond lengths are in good agreement with those reported for *trans-anti*-$[Cr(NCS)_2(Me_2tn)_2]SCN{\cdot}0.5H_2O$ [4], *cis*-$[Cr(NCS)_2(cyclam)]NCS$ [23], *cis*-$[Cr(NCS)_2(cyclam)]_2[Cr_2O_7]{\cdot}H_2O$ [24] and *cis*-[Cr(NCS)(cyclam)(μ-NCS)$ZnCl_3$] [25], respectively. In complex **1**, all the six-membered rings adopt the stable chair conformations and two substituted methyl groups on the carbon of the Me_2tn ligand do not affect the essential features of the six-membered chelate ring. The mean C–N and C–C distances in the Me_2tn ligand are typical and are comparable to those observed for other *trans*-$[CrL_2(Me_2tn)]^+$ ($L = Cl^-, Br^-, NCS^-, N_3^-, CN^-$) complexes with various anions [5-17]. The crystal packing of complex **1** comprises extensive N–H···S, O–H···S and N–H···N hydrogen-bonding interactions among the NH groups of the Me_2tn ligand, OH group of *i*-PrOH and the S atoms of the NCS groups (Table-5). An array of these contacts generate a three dimensional network as shown in Fig. 6. The extensive contacts help to stabilize the crystal structure.

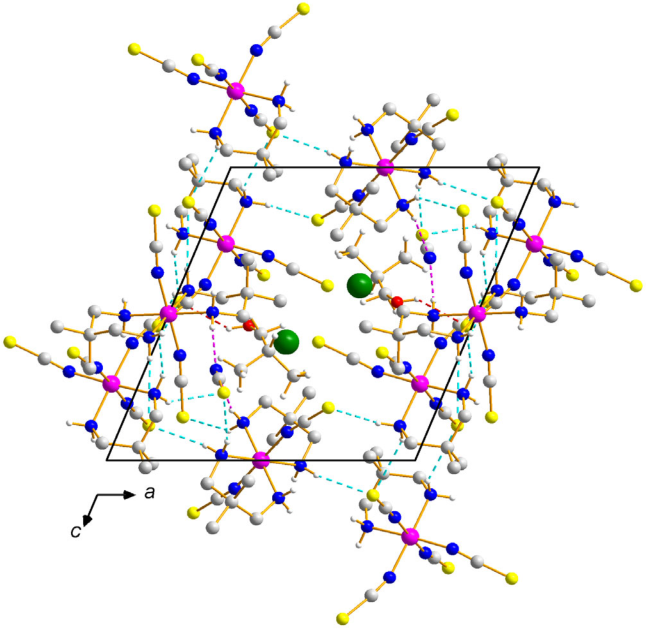

Fig. 6. Crystal packing of complex **1** as seen along the *b* direction. Dashed lines represent N—H···N (pink), O—H···S (red) and N—H···S (cyan) hydrogen bonds, respectively

TABLE-5
HYDROGEN BOND PARAMETERS (Å,°) FOR COMPLEX **1**

D–H···A	D–H	H···A	D···A	D–H···A
N1B—H1B2···N1S	0.92	2.22	3.112(3)	162.8
N1B—H1B2···S2S	0.92	2.52	3.342(12)	148.7
N1C—H1C1···S2B	0.92	2.64	3.4603(19)	149.6
N1A—H1A1···S4F^{i}	0.92	2.79	3.483(5)	133.3
N1A—H1A1···S4C^{i}	0.92	2.92	3.537(3)	125.3
N1A—H1A2···N1S^{ii}	0.92	2.07	2.956(3)	162.1
N1A—H1A2···S2S^{ii}	0.92	2.33	3.198(11)	158.4
N2A—H2A1···S2C^{iii}	0.92	2.64	3.487(6)	152.7
N2A—H2A1···S2F^{iii}	0.92	2.70	3.500(5)	145.3
N2A—H2A2···S3C^{iii}	0.92	2.90	3.779(3)	159.4
N1B—H1B1···S1A^{iv}	0.92	2.70	3.498(2)	146.2
N1B—H1B1···S1D^{iv}	0.92	2.76	3.54(2)	143.1
N2B—H2B1···S3C^{v}	0.92	2.60	3.480(3)	161.1
N1C—H1C2···S3C^{v}	0.92	2.81	3.5202(17)	134.9
N2B—H2B2···N2S^{vi}	0.92	2.36	3.15(3)	145.0
N2B—H2B2···S1S^{vi}	0.92	2.54	3.3971(19)	156.2
N2C—H2C1···N2S^{vii}	0.92	2.14	2.99(3)	153.9
N2C—H2C1···S1S^{vii}	0.92	2.62	3.4097(18)	143.9
N2C—H2C2···S2F^{viii}	0.92	2.64	3.469(11)	149.6
N2C—H2C2···S2C^{viii}	0.92	2.80	3.603(6)	146.0
O1I—H1I···S2C^{ix}	0.84	2.81	3.438(6)	132.6

Symmetry codes: (i) –x+1, –y+2, –z+1; (ii) x, y+1, z; (iii) –x+1, –y+1, –z+1; (iv) x, y–1, z; (v) –x+2, –y+1, –z+2; (vi) –x+1, –y+1, –z+2; (vii) x+1, y, z; (viii) –x+2, –y+1, –z+1; (ix) x–1, y, z.

Conclusion

A new double chromium(III) complex, *trans*-$[Cr(NCS)_2(Me_2tn)_2][Cr(NCS)_4(Me_2tn)]{\cdot}NaSCN{\cdot}$*i*-PrOH, (**1**) has been synthesized and characterized by physical properties and single-crystal X-ray diffraction analyses. The infrared spectroscopic properties of newly synthesized complex **1** were in agreement with the X-ray crystallographic data, which shows that chromium atoms were in a distorted octahedral environment, coordinated by two bidentate, 2-dimethyl-1,3-diaminopropane ligands and two N-bonded NCS ligands in *trans* positions. The carbon atoms of the two chelate rings in two crystallographically independent chromium(III) complex cations were on opposite sides (*anti*) of the Me_2tn coordination plane not including *syn*-conformer. The crystal lattice was stabilized by the hydrogen-bonding interactions among the NH groups of the Me_2tn ligand, OH group of *i*-PrOH and the S-atoms of the NCS groups. The crystal packing force, hydrogen bond types, co-crystalized salt and solvated molecule, as well as the counter anion dimensions, significantly influenced the formation of different conformations.

ACKNOWLEDGEMENTS

This work was supported by a grant from the 2020 Research Fund of Andong National University. The X-ray crystallography experiment at the PLS-II BL2D-SMC beamLine was supported in part by MSIT and POSTECH.

CONFLICT OF INTEREST

The authors declare that there is no conflict of interests regarding the publication of this article.

REFERENCES

1. D.A. House, *Inorg. Chem.*, **25**, 1671 (1986); https://doi.org/10.1021/ic00230a029
2. M.F. DaCruz and M. Zimmer, *Inorg. Chem.*, **35**, 2872 (1996); https://doi.org/10.1021/ic9512237
3. (a) K. Nakamoto, Infrared and Raman Spectra of Inorganic and Coordination Compounds, Part A: Theory and Applications in Inorganic Chemistry, John Wiley & Sons; New York, ed. 6 (2009); (b) K. Nakamoto, Infrared and Raman Spectra of Inorganic and Coordination Compounds, Part B: Applications in Coordination, Organometallic, and Bioinorganic Chemistry, John Wiley & Sons; New York, ed. 6, (2009).
4. J.-H. Choi and S.H. Lee, *J. Mol. Struct.*, **932**, 84 (2009); https://doi.org/10.1016/j.molstruc.2009.05.048
5. J.-H. Choi, S.H. Lee and U. Lee, *Acta Crystallogr. Sect E*, **64**, m1429 (2008); https://doi.org/10.1107/S1600536808032911
6. D. Moon and J.-H. Choi, *Acta Crystallogr. Sect C*, **71**, 351 (2015); https://doi.org/10.1107/S2053229615006026
7. J.-H. Choi, T. Joshi and L. Spiccia, *Z. Anorg. Allg. Chem.*, **637**, 1194 (2011); https://doi.org/10.1002/zaac.201100029
8. D. Moon and J.-H. Choi, *Spectrochim. Acta A Mol. Biomol. Spectrosc.*, **138**, 774 (2015); https://doi.org/10.1016/j.saa.2014.11.099
9. D. Moon, C.S. Lee, K.S. Ryoo and J.-H. Choi, *Bull. Korean Chem. Soc.*, **35**, 3099 (2014); https://doi.org/10.5012/bkcs.2014.35.10.3099
10. D. Moon, J.-H. Choi, *Inorg. Chim. Acta*, **519**, 120259 (2021); https://doi.org/10.1016/j.ica.2021.120259
11. J.-H. Choi, W. Clegg, G.S. Nichol, S.H. Lee, Y.C. Park and M.H. Habibi, *Spectrochim. Acta A Mol. Biomol. Spectrosc.*, **68**, 796 (2007); https://doi.org/10.1016/j.saa.2007.01.002
12. D. Moon, C.S. Lee and J.-H. Choi, *J. Chem. Crystallogr.*, **44**, 306 (2014); https://doi.org/10.1007/s10870-014-0515-5
13. J.-H. Choi, T. Suzuki and S. Kaizaki, *Acta Crystallogr. Sect C*, **58**, m539 (2002); https://doi.org/10.1107/s0108270102018231
14. D. Moon and J.-H. Choi, *J. Mol. Struct.*, **1177**, 338 (2019); https://doi.org/10.1016/j.molstruc.2018.09.049
15. D. Moon, M.A. Subhan and J.-H. Choi, *Int. J. Chem. Sci.*, **14**, 1829 (2016).
16. J.W. Shin, K. Eom and D. Moon, *J. Synchrotron Radiat.*, **23**, 369 (2016); https://doi.org/10.1107/S1600577515021633
17. Z. Otwinowski and W. Minor, eds., C.W. Carter Jr. and R.M. Sweet, Methods in Enzymology, Academic Press: New York, Macromolecular Crystallography, Part A, vol. 276, pp. 307-326 (1997).
18. G.M. Sheldrick, *Acta Crystallogr. Sect A*, **71**, 3 (2015); https://doi.org/10.1107/S2053273314026370
19. G.M. Sheldrick, *Acta Crystallogr. Sect C*, **71**, 3 (2015); https://doi.org/10.1107/S2053229614024218
20. K. Brandenburg and H. Putz, DIAMOND-3, University of Bonn, Germany (2014).
21. J.-H. Choi, *Inorg. Chim. Acta*, **362**, 4231 (2009); https://doi.org/10.1016/j.ica.2009.05.024
22. J.-H. Choi, I.G. Oh, T. Suzuki and S. Kaizaki, *J. Mol. Struct.*, **694**, 39 (2004); https://doi.org/10.1016/j.molstruc.2004.01.034
23. D. Moon, J.-H. Choi, K.S. Ryoo and Y.P. Hong, *Acta Crystallogr. Sect E*, **69**, m376 (2013); https://doi.org/10.1107/S1600536813015456
24. D. Moon, S. Tanaka, T. Akitsu and J.-H. Choi, *Acta Crystallogr. Sect E*, **73**, 72 (2017); https://doi.org/10.1107/S2056989016020120
25. D. Moon and J.-H. Choi, *J. Coord. Chem.*, **74**, (2021) in press; https://doi.org/10.1080/00958972.2020.1863381